

Parameter Analysis of Convolutional Neural Network Operated on Embedded Platform for Estimation of Combustion Efficiency in Coal Burners

Veysel GÜNDÜZALP^{1*}, Gaffari ÇELİK², Muhammed Fatih TALU³, Cem ONAT⁴

^{1,3} Inonu University, Faculty of Engineering, Department of Computer Engineering, Malatya, Türkiye

² Agri Ibrahim Cecen University, Vocational School, Department of Computer Technology, Ağrı, Türkiye

⁴ Adıyaman University, Faculty of Engineering, Department of Mechanical Engineering, Adıyaman, Türkiye

Veysel GÜNDÜZALP ORCID No: 0000-0002-9199-5749

Gaffari ÇELİK ORCID No: 0000-0001-5658-9529

Muhammed Fatih TALU ORCID No: 0000-0003-1166-8404

Cem ONAT ORCID No: 0000-0002-4295-4860

*Corresponding author: vgunduzalp@gmail.com

(Received: 17.10.2022, Accepted: 16.05.2023, Online Publication: 22.06.2023)

Keywords

Coal,
Combustor,
Combustion
Efficiency,
Image
Processing,
Convolutional
Neural Networks

Abstract: Accurately and effectively calculating combustion efficiency in coal burners is crucial for industrial boiler manufacturers. Two main approaches can be used to calculate boiler efficiency: 1) Analyzing the gas emitted from the flue; 2) Visualizing the combustion chamber in the boiler. Flue gas analyzers, which are not user-friendly, come with high costs. Additionally, the physical distance between the flue and the combustion chamber causes the measurement to be delayed. Methods based on visualizing the combustion chamber do not have these disadvantages. This study proposes a system based on visualizing the combustion chamber and has two contributions to the literature: 1) for the first time, the modern Convolutional Neural Networks (CNN) approach is used to estimate combustion efficiency; 2) the CNN architecture with optimal parameters can work on an embedded platform. When classical classification techniques and a CPU-supported processor card are used, efficiency can be calculated from one flame image in 1.7 seconds, while this number increases to approximately 20 frames per second (34 times faster) when the proposed CNN architecture and GPU-supported processor card are used. The results obtained demonstrate the superiority of the proposed CNN architecture and hardware over classical approaches in estimating coal boiler combustion efficiency.

Kömür Yakıcılarında Yanma Verimi Tahmini için Gömülü Platformda Çalışabilen Evrişimsel Sinir Ağının Parametre Analizi

Anahtar Kelimeler

Kömür,
Yakıcı Sistem,
Yanma Verimi,
Görüntü İşleme,
Evrişimsel Sinir
Ağları

Öz: Kömür yakıcılarında yanma veriminin doğru ve etkin bir şekilde hesaplanması endüstriyel kazan üreticileri için oldukça önemlidir. Kazan veriminin hesaplanabilmesi için iki temel yaklaşımın olduğu görülmektedir: 1) bacadan çıkan gazın analizi; 2) kazandaki yanma odasının görüntülenmesi. Kullanımı yeterince kolay olmayan baca gazı analizörleri yüksek maliyete sahiptir. Ayrıca baca ile yanma odası arasındaki fiziksel uzaklık yapılan ölçümün zaman gecikmeli olmasına neden olmaktadır. Yanma odasının görüntülenmesine dayalı yöntemler bahsedilen dezavantajları içermemektedir. Bu çalışmada önerilen ve yanma odasının görüntülenmesine dayanan sistemin literatüre iki katkısı bulunmaktadır: 1) yanma veriminin tahmininde ilk defa modern evrişimsel sinir ağları (ESA) yaklaşımının kullanılması; 2) Optimum parametrelere sahip ESA mimarisinin gömülü bir platformda çalışabilmesi. Klasik sınıflandırma teknikleri ve CPU destekli bir işlemci kartı kullanıldığında, 1,7 saniyede 1 adet alev formu görüntüsünden verim hesaplanabilirken, önerilen ESA mimarisi ve GPU destekli bir işlemci kartı kullanıldığında bu sayı saniyede yaklaşık 20 adet seviyesine çıkmaktadır (34 kat hızlı). Elde edilen sonuçlar, kömür kazanı yanma verimi tahmininde önerilen ESA mimarisinin ve donanımının klasik yaklaşımlara olan üstünlüğünü açık bir şekilde ortaya koymaktadır.

1. INTRODUCTION

The increase in the combustion efficiency of the coal boiler is of great importance for human health, as it causes a decrease in carbon dioxide emissions [1]. In addition, the increase in efficiency provides economic benefits to the enterprises as it will cause the targeted heat energy to be met with less amount of coal.

Classical approaches use the outputs of flue gas analyzers to calculate boiler efficiency [2]. Designers have generally chosen to reduce the oxygen concentration in the flue gas for better efficiency. Many researchers aimed to reduce NO_x emissions in coal boilers and tried different optimization techniques to achieve this. It is in the subcategory of flue gas inspection for low NO_x emissions. Lee and Jou reduced the oxygen concentration of the gas in the chimney by 1% to increase the combustion efficiency by 0.6% [3]. Hao et al. used a genetic algorithm (GA) and artificial neural network (ANN) to optimize NO_x emission in boilers using powdered coal as fuel [4]. In this study of Hao, genetic algorithms were used to determine the current state to optimize the ANN [5]. In addition, it is possible to see researchers that try to reduce the NO_x level of accidents below the legal level in their countries with ant colonies and genetic algorithm methods [6]. Liu et al. made important studies on boilers using different fuels [7]. In the aforementioned study, wood sawdust was used as fuel. Liu et al. In these studies, an extra air inlet was added to the boiler, and the effect of this inlet on NO_x and CO emissions was observed according to the altitude. Kauprianov et al. gave detailed information about the relationship between heat losses and the density of the gas in the chimney [8].

The studies mentioned above adopt the flue gas analysis approach to increase boiler efficiency. However, there are three disadvantages to using flue gas analyzers: 1) high cost; 2) difficulty of use; 3) time delay. For flue gas analyzers to be used in a coal burner system with a high market price, a hole must be drilled in the chimney and the measuring apparatus (metal rod) must be fixed in the drilled hole. This process creates significant difficulty for the user. In addition, the system's performance is adversely affected due to the time delay. In addition, these devices, which can measure once per second, require special-purpose licensed software.

Another preferred method to understand boiler efficiency is observing the flame form by the technical staff and manually making the necessary interventions. For this, the coal burner's existing combustion chamber inspection hole is used. This method, which is based on human observation, has disadvantages such as human error, forgetting, and failure to intervene promptly.

Observing the flame form using image processing techniques is a cost-effective, fast, easy-to-use, and error-prone method compared to manual or classical flue gas measurement methods. When the studies on the flame are examined, it seems that the first remarkable studies are related to the imaging of the combustion

chamber. With the flame images, the combustion status of the burner system can be monitored instantly. Yamaguchi et al. to understand the response of the system-to-air ratio differences, evaluated the intensity of the flame using sensors [9]. Lino et al. used image processing to determine the movements of the flame [10]. In the aforementioned study, the variation of flame brightness versus time was investigated. Huang et al. studied flame images in detail [11]. Onat [1] et al. carried out studies that could extract the attributes of the flame form and match the air excess coefficient (λ) with artificial learning methods. However, these studies could not go beyond the use of classical feature extraction and classification techniques.

Contrary to classical studies, the use of Convolutional Neural Networks (CNN) is recommended in this article to calculate the yield from the image. Thanks to this approach, feature extraction and classification can be done together. In Fig. 1, the general working principle of the classical and proposed approaches is shown together.

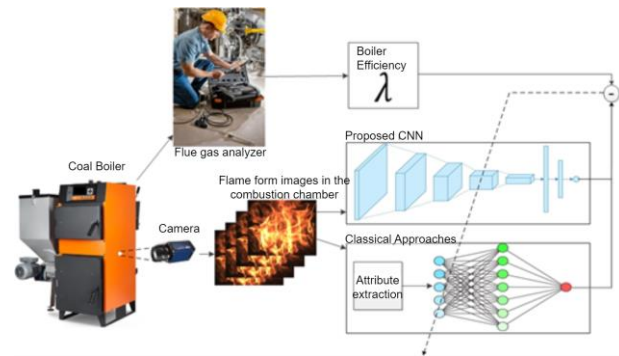


Figure 1. The general operation of the system

2. MATERIAL

The data obtained through a camera placed at the mouth of a boiler, which was positioned to visualize combustion inside the boiler, was used to estimate combustion efficiency from flame images in this study. The combustion section is visualized through the camera placed in the observation section of the boiler. The images are captured as instantaneous 2D images using a CCD camera connected to a computer. The camera has a resolution of 659x494 pixels. As a result, a dataset containing 9965 flame image samples was created. The sample data is presented in Fig. 2.



Figure 2. Sample flame images

3. METHODS

In this section, the classical methods used to extract features from flame form images obtained from the combustion chamber of the coal boiler are expressed. In addition, the proposed convolutional neural network

architecture for the estimation of combustion efficiency is mentioned.

3.1 Classical Feature Extraction Methods

Classical methods such as Hue-Hist, Gray co-occurrence matrix, Blue-Hist, PCA, RES, and Multivariate normal distribution were used to extract the features.

3.1.1 Hue-Hist

Flame form image is obtained in RGB format. Therefore, first RGB→HSV color space conversion is performed and then the histogram of the H channel is obtained. Since the number of parts in the histogram was taken as 255, a 1x255 feature was obtained from each image [12,13].

3.1.2. Gray co-occurrence matrix

The flame from the image in RGB format is converted to gray format and the co-occurrence matrix is calculated. This matrix contains the second-order statistical features of an image. As is known, first-order statistics do not contain any information about the positions of different intensity values in the image. Contains the number of patterns formed by pairs of pixels within a predetermined distance range. This 8x8 matrix contains a total of 1x64 attribute information [14,15].

3.1.3. Blue-Hist

As a result of the studies on the channels of the RGB flame image, it has been seen that it is possible to observe the outer environment of the flame form by using the B channel. This provides important information about the size of the flame form. For this reason, the histogram data of channel B is calculated and a 1x255 feature is obtained [12].

3.1.4. PCA

After the gray conversion of the RGB image is realized, its size is reduced by the PCA method. In the dimension reduction process, the two largest eigenvalues of the gray density matrix are used [16,17].

3.1.5 Radial energy signal (RES)

Radiant energy signal is in the form of waves or particles, mainly in the form of electromagnetic radiation. Heat is an example of radiant energy. The average value of image color intensities is expressed as radiant energy [18,19].

3.1.6. Multivariate normal distribution

The similarity of each pixel in the flame form image to a particular model is calculated. First, the mean and covariance of an image expressing optimal combustion are calculated. Then, the similarity of each pixel in the

newly obtained flame form image to the optimal form is calculated with the following formula [12].

$$Feature[t] = \frac{1}{\sqrt{|\Sigma_k|} (2\pi)^d} \exp\left(-\frac{1}{2} (k_{i,j} - \mu_k) \Sigma^{-1} (k_{i,j} - \mu_k)^T\right) \quad (1)$$

3.2. Proposed CNN Architecture

Since 2012, CNN architectures have dominated the field of machine learning, and most classical image processing and computer vision techniques have been redesigned with these architectures. The success of CNN has been experienced in various fields, particularly in image classification [20], object detection [21], scene classification [22], activity recognition from physical movements [23], Covid-19 detection from X-ray and CT images [24], brain MRI segmentation [25], brain tumor diagnosis [26], ECG arrhythmia classification [27], Covid-19 diagnosis from cough sound [28], Parkinson's disease detection from speech signals [29], etc., significantly improving the performance in these areas. The success of CNN has drawn the attention of many researchers in this direction.

In this study, the flame-efficiency matching accuracy of many different CNN architectures was examined and the parameters of the optimum architecture were determined. The optimum CNN architecture obtained is shown in Table 1. The total number of parameters in the architecture with a 23-layer structure is 219.891. Mean Squared Error (MSE) has been used to update the weights of the proposed architecture [30].

$$Loss_{MSE} = \frac{1}{C} \sum_{i=1}^C (\lambda_i - \lambda'_i)^2 \quad (2)$$

Here, C represents the number of samples, λ_i represents the λ value corresponding to the i th flame, and λ'_i represents the estimated λ value.

Table 1. Optimal CNN architecture

Layer	Size	Parameter
conv2d_1 (Conv2D)	(128, 128, 16)	448
conv2d_2 (Conv2D)	(128, 128, 16)	2320
activation_1 (Activation)	(128, 128, 16)	0
batch_normalization_1 (Batch Normalization)	(128, 128, 16)	64
max_pooling2d_1 (MaxPooling2D)	(64, 64, 16)	0
conv2d_3 (Conv2D)	(64, 64, 16)	2320
activation_2 (Activation)	(64, 64, 16)	0
batch_normalization_2 (Batch Normalization)	(64, 64, 16)	64
max_pooling2d_2 (MaxPooling2D)	(32, 32, 16)	0
conv2d_4 (Conv2D)	(32, 32, 16)	2320
activation_3 (Activation)	(32, 32, 16)	0
batch_normalization_3 (Batch Normalization)	(32, 32, 16)	64
max_pooling2d_3 (MaxPooling2D)	(16, 16, 16)	0
conv2d_5 (Conv2D)	(16, 16, 16)	2320
conv2d_6 (Conv2D)	(16, 16, 16)	2320
activation_4 (Activation)	(16, 16, 16)	0
flatten_1 (Flatten)	(4096)	0
dense_1 (Dense)	(50)	204850
activation_5 (Activation)	(50)	0
batch_normalization_4 (Batch Normalization)	(50)	200
dropout_1 (Dropout)	(50)	0
dense_2 (Dense)	(50)	2550
activation_6 (Activation)	(50)	0
dense_3 (Dense)	(1)	51

4. RESULTS AND DISCUSSION

In this study, a CNN-based architecture has been proposed for predicting combustion efficiency from flame images. 90% of the dataset used was reserved for training and the remaining 10% was used for testing. The proposed architecture was trained for 150 epochs using the Adam optimization algorithm (with $lr=1e-2$). The performance of the architectures was evaluated using the R metric, which is defined as follows [12].

$$R = \left(\frac{\sum_{i=1}^C (\lambda_i - \bar{\lambda})(\lambda'_i - \bar{\lambda}')}{\sqrt{\sum_{i=1}^C (\lambda_i - \bar{\lambda})^2 \sum_{i=1}^C (\lambda'_i - \bar{\lambda}')^2}} \right) \times 100 \quad (3)$$

Here, C represents the number of samples, λ_i represents the λ value corresponding to the i th flame, $\bar{\lambda}$ represents the average of λ_i values, λ'_i represents the estimated value, and $\bar{\lambda}'$ represents the average of λ'_i values.

4.1. Classical Approaches

In this section, image- λ matching accuracies of classical approaches are examined. Firstly, features were obtained from colored flame form images by using the feature extraction methods mentioned (see Table 2). Then, the feature vectors were mapped to the relevant λ coefficient with the ANN method. The obtained accuracy values are shown in Table 2. As can be seen from the results, the highest matching accuracy was obtained with the Multivariate normal distribution method.

Table 2. Classical feature extraction methods and their results

Method	Attribute	Working time	Success
	Count		
Hue-hist (0-255) [13]	255	1.366	77.00
Gray co-occurrence matrix [15]	64	0.901	85.50
Blue-hist (255) [15]	255	1.564	73.10
PCA [17]	2	1.693	70.40
RES [19]	4	1.971	64.20
Multivariate normal distribution	768	0.351	95.10

4.2. Proposed Approach

In this section, the parameters of the optimum CNN architecture that will best match the image- λ are investigated. The answers to the questions listed below were sought to discover the optimal architecture:

- What should be the optimal value of the image resolution to be given as input to the CNN architecture?
- What should be the optimal value of "batch size" in the training process?
- What should be the optimal number of layers in the architecture?

4.2.1. Image resolution effect

In this experimental study, the effect of image size on image- λ matching is analyzed. Accordingly, the input image dimensions of the flame form were converted to 128x128, 64x64, 48x48, and 32x32, and training and testing were carried out using a CNN with the same parameters (number of layers, number of iterations, etc.). The obtained accuracy and time results are given in Table 3. Contrary to the classification problem, the input image size is expected to have a large effect on the output value in the regression problem. When the results in Table 3 were examined, it was seen that the image size had a significant effect on the accuracy and time results. As the size increases, the matching accuracy and time spent by CNN increase. Accordingly, the highest matching accuracy was obtained with the image size of 128x128.

Table 3. Accuracy and time effect of image size

Resolution	Success		Time
	Train	Test	Train(sec)
32x32	93.87	94.45	1400
48x48	96.48	93.56	1800
64x64	93.98	94.67	2100
128x128	97.33	95.55	2400

4.2.2. Pack size effect

It is known that the pattern packet size has a large effect on the direction and speed of convergence. It is known that the patterns are trained one by one (stochastic), in small packages (mini-batch), or as a whole (full batch). In this experimental study, to determine the optimum packet size, the training process was carried out by choosing different packet sizes, provided that the total number of images remained constant. The results obtained are given in Table 4. When the results are examined, it is seen that the most suitable package size is 48. When a package size lower or higher than this value is selected, the accuracy values obtained for the training and test set decrease.

Table 4. The effect of packet size on accuracy and time

Package size	Success		Time
	Train	Test	
16	94.45	90.19	
25	95.14	93.76	
48	97.33	94.67	
100	93.87	82.38	
200	90.24	91.05	

4.2.3. Layer count effect

In this experimental study, the effect of CNN architectures with different layer numbers on image- λ matching accuracy is examined. Accordingly, seven different architectures with different layer numbers were created and the accuracy values in the training/test sets were obtained (see Table 5). When the results were examined, it was seen that the highest accuracy values were achieved with the 23-layer CNN architecture. The detailed version of this architecture, where the total number of parameters is 219.891, is presented in Table 1.

Table 5. The effect of the number of layers

Number of Layers	Success	
	Train	Test
4	64.63	68.87
10	87.92	70.16
16	95.95	92.44
18	91.56	92.03
23	97.33	96.34
33	95.03	90.34
42	86.96	89.56

4.2.4. Google colaboratory

The learning accuracy of CNN is directly proportional to the data size in the training set. The larger the dataset, the higher the accuracy. However, the increase in data size complicates the training process. It is very difficult to train complex CNNs with a large number of parameters. Personal computers cannot provide a solution at this point, and the use of servers becomes mandatory. For this reason, Google Colaboratory service, which is offered free of charge by Google, was used in this study. Thanks to this service, the above-mentioned parameter effects studies were carried out using a server with many libraries installed and an NVIDIA Tesla T4 graphics card.

4.2.5. Embedded platform

In this experimental study, the online performance of image- λ matching is investigated. Accordingly, the matching process was carried out in two different concepts: 1) the classical approach was used on a CPU-supported processor card; 2) the Optimum recommended CNN is used on a GPU-supported processor card. In the experimental study with the first concept, it was seen that each flame image can be mapped to the relevant λ value in 1.7 seconds. On the other hand, when the proposed operating concept is used, it is seen that an average of 20 flame images can be mapped to the λ value in 1 second (see Fig. 3).

```

-----START-----
1. Estimated lambda value of the image: 7.82, Elapsed time: 0.23s
2. Estimated lambda value of the image: 6.78, Elapsed time: 0.11s
3. Estimated lambda value of the image: 6.92, Elapsed time: 0.04s
4. Estimated lambda value of the image: 7.04, Elapsed time: 0.04s
5. Estimated lambda value of the image: 6.90, Elapsed time: 0.04s
6. Estimated lambda value of the image: 7.04, Elapsed time: 0.04s
7. Estimated lambda value of the image: 6.62, Elapsed time: 0.04s
8. Estimated lambda value of the image: 7.01, Elapsed time: 0.04s
9. Estimated lambda value of the image: 8.09, Elapsed time: 0.07s
10. Estimated lambda value of the image: 6.82, Elapsed time: 0.06s
11. Estimated lambda value of the image: 6.39, Elapsed time: 0.04s
12. Estimated lambda value of the image: 6.69, Elapsed time: 0.04s
13. Estimated lambda value of the image: 6.80, Elapsed time: 0.04s
14. Estimated lambda value of the image: 6.88, Elapsed time: 0.04s
15. Estimated lambda value of the image: 9.20, Elapsed time: 0.04s
16. Estimated lambda value of the image: 9.12, Elapsed time: 0.04s
17. Estimated lambda value of the image: 8.76, Elapsed time: 0.05s
18. Estimated lambda value of the image: 8.94, Elapsed time: 0.04s
19. Estimated lambda value of the image: 9.13, Elapsed time: 0.03s
20. Estimated lambda value of the image: 9.24, Elapsed time: 0.03s
21. Estimated lambda value of the image: 9.28, Elapsed time: 0.03s
22. Estimated lambda value of the image: 9.35, Elapsed time: 0.04s
23. Estimated lambda value of the image: 9.79, Elapsed time: 0.04s
24. Estimated lambda value of the image: 9.01, Elapsed time: 0.04s
25. Estimated lambda value of the image: 9.64, Elapsed time: 0.04s
26. Estimated lambda value of the image: 9.81, Elapsed time: 0.04s
27. Estimated lambda value of the image: 9.64, Elapsed time: 0.06s
28. Estimated lambda value of the image: 9.96, Elapsed time: 0.06s
29. Estimated lambda value of the image: 9.81, Elapsed time: 0.03s
30. Estimated lambda value of the image: 8.93, Elapsed time: 0.03s
31. Estimated lambda value of the image: 9.93, Elapsed time: 0.04s
32. Estimated lambda value of the image: 9.39, Elapsed time: 0.04s
33. Estimated lambda value of the image: 9.96, Elapsed time: 0.04s
34. Estimated lambda value of the image: 9.38, Elapsed time: 0.04s
35. Estimated lambda value of the image: 10.06, Elapsed time: 0.05s
36. Estimated lambda value of the image: 9.64, Elapsed time: 0.06s
37. Estimated lambda value of the image: 10.04, Elapsed time: 0.03s
38. Estimated lambda value of the image: 9.98, Elapsed time: 0.03s
39. Estimated lambda value of the image: 9.98, Elapsed time: 0.03s
40. Estimated lambda value of the image: 9.98, Elapsed time: 0.04s
-----END-----

```

Figure 3. Image- λ matching time of the embedded platform (online)

4.3. Matching Results of Best Classical Approach and Optimum CNN Architecture

This section compares the best results of the classical and current approaches. As it will be remembered, the highest matching accuracy among classical approaches was obtained by classifying the multivariate normal distribution features with ANN. The image- λ matching accuracy of the proposed CNN architecture (with optimum parameters) with this method is shown in Fig. 4. Accordingly, the red colored line shows the actual λ value, the green CNN result, and the blue ANN result. As can be seen, the proposed CNN architecture can predict λ with high accuracy. If you pay attention, the CNN architecture also performs the filtering of the result while estimating λ .

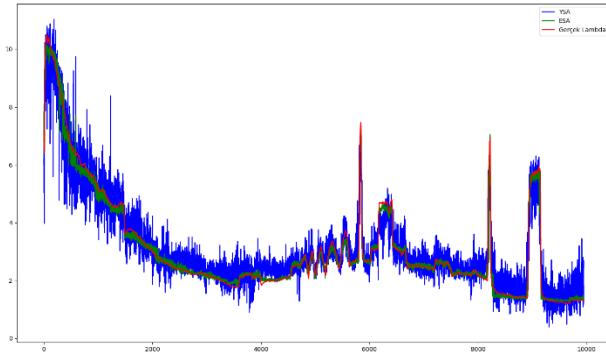


Figure 4. Image- λ matching time of the embedded platform (online)

5. CONCLUSION

In this study, a new method is proposed to calculate the combustion efficiency of coal boilers. This method involves viewing the combustion chamber via a camera and mapping the relevant images to the efficiency coefficient λ taken from a flue gas analyzer. The proposed approach has two important differences from previous image- λ matching studies: 1) CNN architecture is used; 2) Optimum CNN architecture is run on an embedded platform.

As a result of the experimental studies, it has been observed that the flame images can be mapped to the λ coefficients with the highest accuracy (97% for training, 94% for testing) when the following parametric values are used.

- The flame from the image resolution should be 128x128.
- Pack size 48 should be selected in the training process.
- CNN architecture should have 23 layers.

REFERENCES

- [1] Onat C, Talu MF, Daskin M, Mercimek M. Otomatik Beslemeli Kömür Kazanlarında Alev Formu İle Yanma Verimi Arasındaki İlişkinin İncelenmesi. *Mühendis ve Makine* 2015; 669: 70–79, 2015.
- [2] Testo SE, KGaA Co. Baca gazı ölçüm cihazları. 2019 [cited 2019 October 30. Available from: <https://www.testo.com/tr-TR/ueruenler/gaz-oelcuem-cihazlatri>.
- [3] Lee CL, Jou CJG. Saving fuel consumption and reducing pollution emissions for industrial furnaces. *Fuel Process. Technol.* 2011; 92(12):2335–2340.
- [4] Hao Z, Kefa C, Jianbo M. Combining neural network and genetic algorithms to optimize low NOx pulverized coal combustion. *Fuel*: 2011; 80 (15): 2163–2169.
- [5] Hao Z, Qian X, Cen K, Jianren F. Optimizing pulverized coal combustion performance based on ANN and GA. *Fuel Process. Technol.* 2004; 85 (2–3):113–124.
- [6] Zheng Z, Yao M. Charge stratification to control HCCI: Experiments and CFD modeling with n-heptane as fuel. *Fuel*. 2009; 88(2): 354–365.
- [7] Liu D, Yan J, Wang F, Huang Q, Chi Y, Cen K. Experimental reconstructions of flame temperature distributions in laboratory-scale and large-scale pulverized-coal fired furnaces by inverse radiation analysis. *Fuel*. 2012; 93: 397–403.
- [8] Kuprianov V, Chullabodhi C, Jornjumrus W. Cost based optimization of excess air for fuel oil/gas-fired steam boilers. *RERIC Int. Energy J.*1999; 21(2): 83–91.
- [9] Yamaguchi T, Grattan KTV, Uchiyama H, Yamada T. A practical fiber optic air-ratio sensor operating by flame color detection. *Rev. Sci. Instrum.* 1997; 68(1): 197–202.
- [10] Lino N, Tsuchino F, Yano T. TIMEWISE VARIATION OF TURBULENT JET DIFFUSION FLAME SHAPE BY MEANS OF IMAGE PROCESSING. *J. Flow Vis. Image Process.*1998; 5(4): 275–281.
- [11] Huang Y, Yan Y, Lu G, Reed A. On-line flicker measurement of gaseous flames by image processing and spectral analysis. *Meas. Sci. Technol.* 1999; 10(8): 726–733.
- [12] Golgiyaz S, Talu MF, Daşkın M, Onat C. Estimation of excess air coefficient on coal combustion processes via gauss model and artificial neural network. *Alexandria Eng. J.*2022; 61(2): 1079–1089. doi: 10.1016/j.aej.2021.06.022.
- [13] Baek WB, Lee SJ, Baeg SY, Cho CH. Flame image processing & analysis for optimal coal firing of thermal power plant. *ISIE 2001 IEEE Int. Symp. Ind. Electron. proceedeing, Vols I-III.* 2001; 928-931.
- [14] Eleyan A, Dem H. Co-occurrence matrix and its statistical features as a new approach for face recognition. *Comp Sci.* 2011; 19(1).
- [15] TALU MF, ONAT C, DASKIN M. Prediction of Excess Air Factor in Automatic Feed Coal Burners by Processing of Flame Images. *Chinese J. Mech. Eng.* 2017; 30(3): 722–731.
- [16] Chen LC, Papandreou G, Schroff F, Adam H. Rethinking Atrous Convolution for Semantic Image Segmentation. 2017. arXiv:1706.05587
- [17] Chen J, Chan LLT, Cheng YC. Gaussian process regression based optimal design of combustion systems using flame images. *Appl. Energy.* 2013; 111: 153–160.
- [18] Huang B, Luo Z, Zhou H. Optimization of combustion based on introducing radiant energy signal in pulverized coal-fired boiler. *Fuel Process. Technol.* 2010; 91(6): 660–668. doi: 10.1016/j.fuproc.2010.01.015.
- [19] Huang B, Luo Z, Zhou H. Optimization of combustion based on introducing radiant energy signal in pulverized coal-fired boiler. *Fuel Process. Technol.* 2010; 91(6): 660–668.
- [20] Krizhevsky A, Sutskever I, Hinton GE. ImageNet Classification with Deep Convolutional Neural Networks. 2012; 25(2). doi:10.1145/3065386.
- [21] Girshick R, Donahue J, Darrell T, Malik J. Rich feature hierarchies for accurate object detection and semantic segmentation. Nov. 2013.

- [22] Farabet C, Couprie C, Najman L, LeCun Y. Learning Hierarchical Features for Scene Labeling. *IEEE Trans. Pattern Anal. Mach. Intell.* 2013; 35 (8): 1915–1929.
- [23] ÇALIŞAN M, TALU MF. Comparison of Methods for Determining Activity from Physical Movements. *J. Polytech.* 2020; 0900(1): 17–23.
- [24] Celik G. Detection of Covid-19 and other pneumonia cases from CT and X-ray chest images using deep learning based on feature reuse residual block and depthwise dilated convolutions neural network. *Appl. Soft Comput.* 2023; 133: 109906. doi: 10.1016/j.asoc.2022.109906.
- [25] Çelik G, Talu MF. A new 3D MRI segmentation method based on Generative Adversarial Network and Atrous Convolution,. *Biomed. Signal Process. Control.* 2022; 71: 103155. doi: 10.1016/j.bspc.2021.103155.
- [26] Başaran E. A new brain tumor diagnostic model: Selection of textural feature extraction algorithms and convolution neural network features with optimization algorithms. *Comput. Biol. Med.* 2022; 148: 105857. doi: 10.1016/j.compbiomed.2022.105857.
- [27] Rawal V, Prajapati P, Darji A. Hardware implementation of 1D-CNN architecture for ECG arrhythmia classification. *Biomed. Signal Process. Control.* 2023; 85: 104865. doi: 10.1016/j.bspc.2023.104865.
- [28] Hamdi S, Oussalah M, Moussaoui A, Saidi M. Attention-based hybrid CNN-LSTM and spectral data augmentation for COVID-19 diagnosis from cough sound. *J. Intell. Inf. Syst.* 2022; 59(2): 367–389. doi: 10.1007/s10844-022-00707-7.
- [29] Polat K, Nour M. Parkinson disease classification using one against all based data sampling with the acoustic features from the speech signals. *Med. Hypotheses.* 2020; 140:109678. doi: 10.1016/j.mehy.2020.109678.
- [30] Golgiyaz S, Talu MF, Onat C. Artificial neural network regression model to predict flue gas temperature and emissions with the spectral norm of flame image. *Fuel*, 2019; 255: 115827. doi: 10.1016/j.fuel.2019.115827.